Environmental Technology & Innovation 22 (2021) 101508

Contents lists available at ScienceDirect

Environmental Technology & Innovation

journal homepage: www.elsevier.com/locate/eti

Proof of concept: Integrated membrane distillation-forward osmosis approaches water production in a low-temperature CO_2 capture

Lei Zheng [a,b], Kangkang Li [c], Qilin Wang [a], Gayathri Naidu [a], William E. Price [d], Xiwang Zhang [e], Long D. Nghiem [a,f,*]

[a] Centre for Technology in Water and Wastewater, University of Technology Sydney, Ultimo NSW 2007, Australia
[b] Chongqing Institute of Green and Intelligent Technology, Chinese Academy of Sciences, Chongqing 400714, PR China
[c] CSIRO Energy, 10 Murray Dwyer Circuit, Mayfield West, NSW 2307, Australia
[d] Strategic Water Infrastructure Laboratory, School of Chemistry and Molecular Biosciences, University of Wollongong, NSW 2522, Australia
[e] Department of Chemical Engineering, Monash University, Clayton, VIC 3800, Australia
[f] NTT Institute of Hi-Technology, Nguyen Tat Thanh University, Ho Chi Minh City, Viet Nam

ARTICLE INFO

Article history:
Received 7 February 2021
Received in revised form 12 March 2021
Accepted 13 March 2021
Available online 23 March 2021

Keywords:
CO_2 capture
Flue gas
Membrane distillation
Forward osmosis
Monoethanolamine
Sodium glycinate

ABSTRACT

This study investigated the removal of CO_2 from flue gas by an integrated membrane distillation-forward osmosis (MD–FO) system. Monoethanolamine (MEA) and sodium glycinate solutions were loaded with CO_2 from a mixture of CO_2 and N_2 (1:9 in volume ratio) to simulate synthetic flue gas. CO_2 desorption from the amine solution was evaluated using MD at 80 °C. Interaction between amines and the membrane polymeric matrix could alter the membrane surface hydrophobicity; however, under all experimental conditions it was still sufficiently hydrophobic for MD operation. Amine loss during MD operation for CO_2 desorption was insignificant. FO was used to provide make-up water and cooling to the regenerated amine solution after CO_2 desorption by MD. The results showed stable FO water flux when wastewater effluent was used as the source for make-up water. Repetitive CO_2 loading and desorption experiments showed 87.0% and 88.1% CO_2 re-absorption efficiency for MEA and sodium glycinate in the second cycle, respectively. Further investigation of this hybrid system is suggested to advance the CO_2 desorption by MD process and water production by FO process.

1. Introduction

CO_2 removal from flue gas for storage or beneficial utilisation is a pragmatic solution while non fossil-based energy alternatives are still being developed. Fossil fuel combustion produced 37.15 Gt of CO_2, equivalent to 45% of the global green house gas emission (Peters et al., 2019). To reduce green house gas emission from the combustion of fossil fuel, strategies for CO_2 capture from flue gas such as absorption (Liu et al., 2019), membrane separation (Xie et al., 2019; Zhao et al., 2016; Luis et al., 2012) and adsorption (Li et al., 2016b, 2019; Barzagli et al., 2019) have been extensively studied in recent years. Amine-based post-combustion CO_2 capture is a mature technology that can be retrofitted to existing

* Corresponding author at: Centre for Technology in Water and Wastewater, University of Technology Sydney, Ultimo NSW 2007, Australia.
E-mail address: Duclong.Nghiem@uts.edu.au (L.D. Nghiem).

https://doi.org/10.1016/j.eti.2021.101508
2352-1864/

power stations. Examples of power stations retrofitted with amine-based post-combustion CO_2 capture include Boundary Dam (Stéphenne, 2014) and Petra Nova (Petra Nova - W.A. Parish Project in, 2018).

Monoethanolamine (MEA) is the most widely used chemical for amine-based CO_2 capture due to features such as high absorption capacity, fast reaction kinetics and high mass transfer. Apart from MEA, several amino acid salts such as sodium glycinate have also gained scientific and commercial attention because of their greater resistances to oxidative degradation and lower toxicity than MEA (Zhang et al., 2018; Moioli et al., 2019). These amino acid salts have an amine group and an acidic carboxylic acid group, which can be protonated, neutral, or deprotonated as a function of pH (Guo et al., 2013). The zwitterionic mechanism is often considered to interpret the chemical reaction between CO_2 and solvents (Caplow, 1968; Lv et al., 2015). In this mechanism, a primary or secondary amino group of amines firstly reacts with CO_2 to form a zwitterion (Eq. 1). The base (i.e. amine, OH^-, or H_2O) neutralises the intermediate to form a carbamate (Eq. 2). These carbamates can be thermally reversed back to amine and CO_2via the following reactions:

$$CO_2 + RNH_2 \leftrightarrow RNH_2^+COO^- \quad \text{(Eq. 1)}$$

$$RNH_2^+COO^- + RNH_2 \leftrightarrow RNHCOO^- + RNH_3^+ \quad \text{(Eq. 2)}$$

In the current amine-based CO_2 removal process, amine solution is regenerated by a stripping with steam at about 120 °C. This thermal energy consumption accounts for about 75% of the overall costs because of large amount of steam used for the absorbent regeneration (Singh and Versteeg, 2008; Idem et al., 2006) and Rochelle (2009). In addition, the high stripping temperature resulted in thermal degradation and subsequent amine loss (Vevelstad et al., 2011). Recent approaches to address these drawbacks focus on the absorbent formulation and process innovation to improve the CO_2 capture performance, such as solvent modification with promoters, efficient gas–liquid contactors, microwave swing regeneration and, electrochemically mediated amine regeneration (Li et al., 2020; McGurk et al., 2017; Dutcher et al., 2013). For example, Li et al. (Cheng et al. (2018), Li et al. (2018)) observed that addition of metal ions (i.e. Cu and Me) in the aqueous amine solution could enhance the CO_2 desorption rate and reduce the heat of CO_2 desorption, thus reducing the regeneration energy. However, these approaches still rely on high temperature CO_2 desorption, and have not been realised at full scale for CO_2 capture. Another inherent disadvantage of high temperature CO_2 desorption is the high energy demand for cooling. The large water demand for the trim cooler is a major hurdle for inland CO_2 capture plants where fresh water is scarce.

New research effort has been devoted to technologies with low CO_2 desorption temperature so that the low-grade waste heat from the power plants can be utilised. In the US alone, thermal power plants discharge 18.9 billion GJ_{th}waste heat each year at temperature around 85 °C (Gingerich and Mauter, 2015). If fully utilised this waste heat can offset most of the thermal energy requirement for CO_2 capture.

The CO_2 desorption kinetics from an amine solution is slow. However, the rate of CO_2 desorption can be improved by removing or reducing water activities in the system. Lin and Wong (2014) lowered the water activity by adding methanol into a water-amine system and observed 67% higher CO_2 desorption at 80 °C than that of MEA only at 120 °C in terms of the cyclic loading performance. Lai et al. (2019) also observed higher CO_2 desorption rate in an alcohol-amine-water system than that of a single amine system. In the 40 wt% ethanol/20 wt% MEA solution, CO_2 desorption rate was reported to increase by more than 6 times, from 0.021 to 0.137 mmol/s. This may be attributed to dielectric constant compression of amine due to alcohol addition and therefore reduced the basic strength of the sorbent, which helped to release acidic CO_2 at a low temperature (Hamborg et al., 2010). Barzagli et al. (Barzagli et al. (2013) and Barzagli et al. (2018)) reported that MEA was more stable than other secondary amines (e.g. amines 2-2(2-aminoethoxy)ethanol) with more residual carbamates at 110 °C desorption by ^{13}C NMR spectroscopy. They also observed that a mixture of amines (i.e. alkanolamine and 2-amino-2-methyl-1-propanol) could achieve 73–96% efficiency at the low desorption temperature (< 90 °C). Another approach is to remove water from the system during CO_2 desorption, which can also increase CO_2 desorption rate.

Membrane distillation (MD) can utilise low-grade heat and remove water at the same time, enabling MD a good candidate for the low temperature CO_2 desorption. Unlike pressure driven membrane technologies (such as nanofiltration and reverse osmosis), MD is a thermally driven separation process. The difference in partial water vapour pressure across a microporous and hydrophobic membrane induced by temperature difference between the feed and distillate side is the driving force of the MD process (Wang and Chung, 2015; Naidu et al., 2020). The membrane surface properties can be precisely controlled to achieve anti-fouling and anti-wetting properties (Jia et al., 2020; Ray et al., 2018; Xiao et al., 2020).

MD is operated at well below the water boiling temperature. Thus, the low-grade heat from power plants can be directly utilised in MD process to regenerate the amine solution after heat exchanger at 80 °C or below. MD can remove water from the water-amine solution to improve the rate of CO_2 desorption. MD has been successfully demonstrated at pilot scale for further removal of water from hypersaline solutions (Duong et al., 2015; Song et al., 2008). Several studies have also demonstrated the potential of low-temperature CO_2 desorption from amine and amino acid salt by hollow fibre membrane contactors (McGurk et al., 2017; Rahim et al., 2015; Zhao et al., 2015). However, to date, the feasibility of MD for low-temperature (∼80 °C) CO_2 desorption has not been systematically investigated.

In the amine-based CO_2 capture process, after regeneration, it is necessary to cool down the amine solution to a desired CO_2 absorption temperature and compensate to the corresponding water loss from the CO_2 desorption. Previous

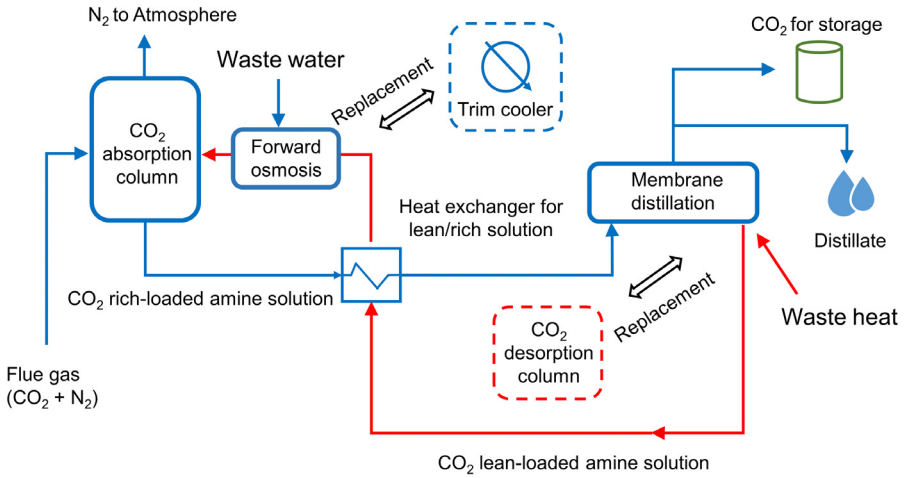

Fig. 1. Conceptual integrated MD–FO process flow diagram. The process includes two stages: (1) CO_2 desorption supplement by membrane distillation for low temperature operation; and (2) Forward osmosis to replace a trim cooler.

Table 1
Specifications of hydrophobic membranes used in this study.

Membrane	Supplier	Thickness (μm)	Porosity (%)	Pore size (μm)
1	General Electric (US)	179	75	0.22
2	Porous Membrane Technology (China)	60	80	0.2

studies (Feron et al., 2017; Gwak et al., 2019; Zheng et al., 2020) have demonstrated the potential of forward osmosis (FO) for simultaneous cooling of the regenerated amine solution and providing make-up water.

In this study, we propose an integrated MD–FO system to simultaneously achieve two objectives: (1) CO_2 desorption at low temperature; (2) cooling and provision of make-up water after desorption. This study aims to extend the previous theoretical framework and to evaluate the effect of membrane material and adsorbent type on the system performance.

2. Materials and methods

2.1. Conceptual diagram of proposed MD-FO for CO_2 capture

Fig. 1 conceptually describes the proposed MD–FO process for low temperature CO_2 capturing from flue gas. Inputs into the process are flue gas and waste heat from coal fired power plants and wastewater. Outputs from the process include purified CO_2 for storage or beneficial use, high quality distillate, and N_2 that can be vented to the atmosphere. Via an adsorption–desorption cycle, pure CO_2 is extracted from flue gas for compression, storage or beneficial use. Wastewater is used as the make-up water via the FO process. Waste heat from the power plant is used to desorb CO_2 (regenerate the amine solution) and produce high quality distillate for beneficial use.

2.2. Membranes and chemicals

Two commercially available flat-sheet hydrophobic polytetrafluoroethylene (PTFE) membranes were used for the MD process (Table 1). A flat-sheet hydrophilic thin film composite (TFC) membrane (Porifera, US) was used for FO process. This TFC membrane consists of a thin active layer and an embedded woven support layer. The operational ranges of pH of these membranes are between 3 and 13, which cover the pH range of the amine solution before and after CO_2 absorption.

Reagent grade MEA, glycine and sodium hydroxide were from Sigma-Aldrich. Sodium glycinate was prepared by mixing glycine with an equal molar ratio between glycine and sodium hydroxide in deionised (DI) water. Instrument grade (>99.8% purity) CO_2 and N_2 gases were from Coregas Australia and stored in pressurised cylinders.

2.3. Feed solution for MD and FO

CO_2 and N_2 gases were mixed together using Bronkhorst mass flow controllers to obtain a CO_2:N_2 gas ratio by volume of 1:9 to simulate the composition of flue gas. Simulated flue gas was constantly bubbled into the 5 L of MEA (5 M) or sodium glycinate (3 M) solution at a flow rate of 1.1 L/min at 40 °C controlled by a water bath. Gaseous CO_2 concentration was analysed by a gas analyser (Horiba, VA-3000) with the analytical range of 0–10 vol% every 15 s. The CO_2 rich solution

was considered fully loaded when CO_2 concentration in the outlet was the same as in the inlet. These CO_2 rich-loaded solutions were used as the feed solution for MD experiment.

CO_2 rich-loaded solutions became CO_2 lean-loaded solution after CO_2 desorption in the MD experiment and CO_2 lean-loaded solutions were used as the draw solution in FO process. As a kind of non-portable water, treated effluent from a membrane bioreactor (Nguyen et al., 2020) was used as the feed solution in FO process. The conductivity and total organic carbon (TOC) of this treated effluent was 5 mS/cm and 7 mg/L. DI water was used as the feed solution in the baseline test with the same draw solution for treated effluent.

2.4. MD for CO_2 desorption and FO for water supplement

The CO_2 desorption experiments for CO_2 rich-loaded solution were performed using a lab-scale direct contact membrane distillation (DCMD) system (Supplementary Data Fig. S1a). The membrane module was in a plate-and-frame configuration with an effective membrane area of 17.5 cm^2. Feed solution (0.5 L) and distillate (2 L) were circulated counter-currently by two gear pumps (Cole Parmer, model 75211-15, US) at the flow rate of 1.0 L/min (corresponding to 36.2 cm/s). In all experiments, the CO_2 rich-loaded feed solution was placed in a jacketed vessel coupled with a temperature control system (Thermoline, model BL-30, Australia) and maintained at 80 $\pm$ 2 °C. 80 °C represents the low-grade power plant waste heat (Novek et al., 2016), which is a reasonably low temperature compared to the conventional regeneration temperature (120 °C). The distillate was maintained at room temperature (25 $\pm$ 2 °C) using another temperature control system (Thermoline, model BL-30, Australia). Inlet and outlet temperature of the feed solution and distillate flow channels were recorded by temperature sensors (Vernier LabQuest 2, US).

The distillate reservoir vessel was placed on a digital balance (Adam, model PGL 8001, Australia) and the weight change was recorded every 3 min and transferred to a data logger. Preliminary experiments showed that CO_2 desorption stopped at water recovery of 30% or more. Samples (2 mL) from the feed solution were collected at 10, 20, and 30% water recovery to monitor the CO_2 desorption performance as a function of water recovery. Feed and distillate samples (50 mL) were also taken at the beginning and end of each experiment for other analyses. Upon the DCMD process, the final concentrated feed solutions were then used as draw solutions for the subsequent FO experiments.

After the CO_2 desorption experiment, the experimental equipment was rearranged into a FO system. The same membrane cell was used for the FO system to provide make-up water and cooling to the CO_2 lean-loaded solution also known as the regenerated amine solution (Supplementary Data Fig. S1b). Draw solution (0.35 L) and feed solution (2 L) were circulated counter-currently. The feed solution reservoir was placed on the digital balance for monitoring the water flux. It is assumed that amine loss during CO_2 desorption did not occur. Thus, each experiment was conducted until the amine solution returned to the initial volume of 0.5 L prior to CO_2 desorption. In other words, the volume of water permeated through the membrane to the CO_2 lean-loaded solution was the same as the volume of clean water produced by MD during CO_2 desorption. Feed solution and draw solution samples (50 mL) were taken at the beginning and end of each experiment for analysis. All DCMD and FO experiments were conducted in duplicate. The results are reported as geometric mean and standard deviation.

2.5. Measurement and analysis

2.5.1. Contact angle measurement

Membrane surface hydrophobicity was determined by contact angle measurement using a goniometer (model: Theta Lite 100, Biolin Scientific, Sweden) and the standard sessile drop method. Five measurements using DI water (5–8 μL) as the reference liquid were conducted at different locations on the membrane surface. Membrane samples were air-dried before contact angle measurement.

2.5.2. Solution chemistry characterisation

The chemical properties of the liquid sample (1 μL) were analysed by using a Fourier transform infrared (FTIR) spectroscopy (model: IRAffinity-1, Shimadzu, Japan) equipped with a single reflection attenuated total reflectance (MIRacle 10, Shimadzu, Japan). Absorbance from wavelength 400 to 4000 cm^{-1} of each sample displayed the corresponding spectra at 4 cm^{-1} resolution. TOC analysis was operated by sparging Non-Purgeable Organic Carbon using a TOC analyser (Analytik Jena Multi N/C 3100, Jena, Germany).

2.5.3. Water flux and reverse salt flux

Water flux (J_w) is an important performance indicator of membrane process, which can be calculated as follow:

$$J_w = \frac{M_{t1} - M_{t2}}{\Delta t \times A \times \rho} \quad (1)$$

where M_{t1} and M_{t2} are the weights of distillate (MD)/feed solution (FO) at time t1 and t2, respectively. Δt is the time interval (3 min); A is the effective membrane area; and ρ is water density.

Due to the constant ratio of carbon for MEA and sodium glycinate, it was possible to carry out TOC analysis to analyse their respective concentration in the solution sample. Reverse salt flux (J_s) indicates the mass diffusion from draw solution to feed solution, which can be calculated based on the mass balance calculation as follow:

$$J_s = \frac{(C_t \times V_{feed,t} - C_0 \times V_{feed,0})}{A \times t} \tag{2}$$

$$V_{feed,t} = V_{feed,0} - \Delta V_{p,t} \tag{3}$$

where $V_{feed,0}$ and $V_{feed,t}$ are the volumes of the feed at the beginning and corresponding time t of the experiment; C_0 and C_t are the concentrations of draw solution in the feed at the beginning and corresponding time t of the experiment, respectively; $\Delta V_{p,t}$ is the volume of distillate at time t. The solute rejection by MD is calculated based on dilution factor ($DF = V_{draw}/\Delta V_{p,t}$) as follow:

$$R(\%) = \left(1 - \frac{DF \times C_{distillate}}{C_{feed}}\right) \times 100 \tag{4}$$

Water recovery (R_w) of MD/FO experiment is defined as the volume fraction of feed that is recovered as permeate:

$$R_w = \frac{Q_p}{Q_F} \tag{5}$$

where Q_p represents the volume of water production, Q_F denotes the volume of feed.

2.5.4. CO_2 loading ratio analysis

The CO_2 loading ratio (α, mol of CO_2/mol of amine) values after absorption and desorption were determined by the excessive acid method (Aroonwilas and Tontiwachwuthikul, 1998). By adding an excess amount of strong acid (i.e. 2 mol/L H_2SO_4) to the liquid sample, CO_2 in the liquid sample was released into the gas phase and precisely measured by the variable volume in a burette.

$$\alpha = \frac{V_{CO_2}}{22.4 \times V_L \times m} \times \frac{P}{P_0} \times \frac{273}{t} \tag{6}$$

where V_{CO_2} denotes the measured volume of released CO_2 from the sample, mL; V_L represents sample volume, mL; m denotes the molar concentration of sample, mol/L; P/P_0 stands for the ratio between room atmospheric pressure and standard atmospheric pressure; t is the room temperature, K. In addition, the accuracy of this method was validated by using different concentrations of sodium carbonate (0.5, 1, and 2 M) aqueous solutions.

The CO_2 desorption efficiency, ρ, is obtained by the following equation:

$$\rho(\%) = (1 - \frac{\alpha_f}{\alpha_i}) \times 100 \tag{7}$$

where α_i and α_f represent initial and final loading of CO_2 rich-loaded and lean-loaded amine solutions. On the other hand, CO_2 re-absorption efficiency, η, is used to compare the loading of CO_2 re-absorption solution (α_r) to that of initial CO_2 rich-loaded solution (α_i).

$$\eta(\%) = \frac{\alpha_r}{\alpha_i} \times 100 \tag{8}$$

3. Results and discussions

3.1. DCMD for CO_2 desorption

3.1.1. CO_2 loading

The CO_2 loading ratios for MEA and sodium glycinate were 0.54 and 0.59 mol/mol, respectively. These results are consistent with the literature (Li et al., 2016a; Zhang et al., 2017; Rabensteiner et al., 2014). CO_2 desorption by DCMD was quantified by monitoring the CO_2 content of the feed solution. Fig. 2 shows 32.8 and 32.4% CO_2 desorption for MEA using Membrane 1 and 2, respectively. Faster desorption rate is observed for MEA when water recovery was between 0 and 20% and no further desorption was observed when water recovery reached 30%. As a thermally driven process, CO_2 desorption is sensitive to temperature. In the current state of the art MEA-based CO_2 capture process, up to 50% CO_2 desorption can be achieved but only at a higher temperature (ca. 120 °C).

The changing CO_2 desorption rate could be explained by the decrease in CO_2 partial pressure and solution pH increase. At water recovery below 20%, high CO_2 loading and high CO_2 partial pressure resulted in faster CO_2 release via thermolysis. As the desorption process continued, partial pressure of CO_2 loaded solution decreased, leading to lower CO_2 desorption. CO_2 desorption is pH dependent. At high pH, carbamic acid formed via the reaction between CO_2 and MEA deprotonates to carbamate. The process is reversed when CO_2 is desorbed. As the solution pH increased due to CO_2 desorption, the desorption rate decreased. The desorption temperature used in this study was much lower than in the conventional amine-based CO_2 capture process; thus, the impact of CO_2 partial pressure and pH on the rate of desorption was more

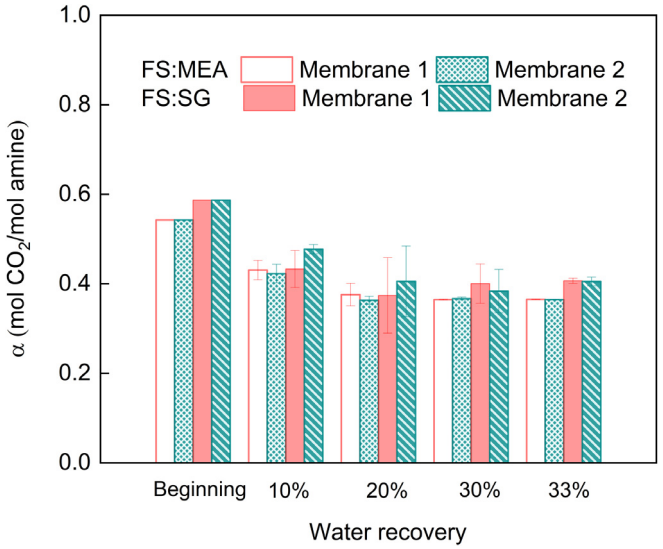

Fig. 2. Loading ratio (α) of CO_2 rich-loaded solution by DCMD as a function of water recovery. Experimental conditions: DI water was used as the distillate. MEA (5 M) and sodium glycinate (SG, 3 M) were used as the feed. The temperatures of the feed solution and distillate were 80 °C and 25 °C respectively. All experiments were conducted in duplicate. The error bars represent the difference between two replicate experiments.

significant. In the conventional process, carbamate was still detectable in the solution after desorption, suggesting that complete regeneration of MEA is impractical (Li et al., 2018).

CO_2 desorption can be also assessed by examining the corresponding pH value of the amine solution. In this study, the pH value of CO_2 rich-loaded MEA was 8.5 and pH increased to 10.7 after desorption (for both membranes). The pH of solution after desorption did not reach the initial value of fresh MEA (12.6), which is consistent with the low desorption efficiency under current experimental condition. Previous works have reported similar CO_2 desorption (32%) from a MEA solution compared to this study under atmospheric pressure but at 120 °C or higher temperature (Lv et al., 2015; Zhao et al., 2017). In practice, 50% desorption efficiency is very desirable but still difficult to be achieved.

The decrease in CO_2 loading in the amine solution in Fig. 2 can be used to quantify CO_2 desorption. CO_2 desorption from a sodium glycinate solution has a similar profile to that of MEA (Fig. 2). Membrane 1 and 2 showed maximum CO_2 desorption efficiency of 36.3% and 34.6%, respectively. CO_2 desorption from MEA solution became negligible when water recovery reached 30%. Similar to MEA, sodium glycinate can also form a stable intermediate via reaction with CO_2 (Song et al., 2012). As water recovery exceeded 20%, no further CO_2 desorption was observed with Membrane 1.

3.1.2. Wettability behaviour after 30% water recovery

The relative wettability of membrane can be determined by contact angle measurement of the membrane surface. There were negligible changes in hydrophobicity for both membranes after desorption experiment using sodium glycinate as the adsorbent (Fig. 3).

Interaction between MEA and membrane polymer could alter the membrane hydrophobicity (Rezaiyan et al., 2017); however, changes in the membrane water contact angle were dependent on the initial hydrophobicity. MEA resulted in a decline in water contact angle of Membrane 1 from 127 to 95°. By contrast, contact angle of Membrane 2 increased by 31% after the desorption experiment using MEA as CO_2 adsorbent (Fig. 3). This improvement was possibly due to the initially low contact angle value of the virgin membrane and membrane swelling caused by the MEA penetration (Ahmad et al., 2018). Despite the variation in water contact angle due to interaction with amine adsorbent, results in Fig. 3 confirm that a sufficiently hydrophobic condition may still be possible for MD operation.

3.1.3. Water activity reduction by DCMD

CO_2 desorption rate can be facilitated by the water reduction in amine solution. Water reduction is represented by the water production in distillate side in terms of water flux in DCMD. Water fluxes during the CO_2 desorption experiment when MEA was used as the absorbent are reported in Fig. 4a. Membrane 1 had an initial flux of 21.2 L/m^2 h, which was stable for only the initial 100 min of the desorption experiment. It then declined to 10.1 L/m^2 h at the end of process possibly due to partial membrane wetting. On the other hand, Membrane 2 showed a more stable water flux throughout the desorption experiment possibly it is thinner and more porous than Membrane 1 (Table 1).

Membrane 1 was thicker (Table 1) but also produced a higher initial water flux than Membrane 2. In the DCMD process, a thick membrane resulted in a higher resistance to mass transfer of water vapour but also prevent unnecessary thermal

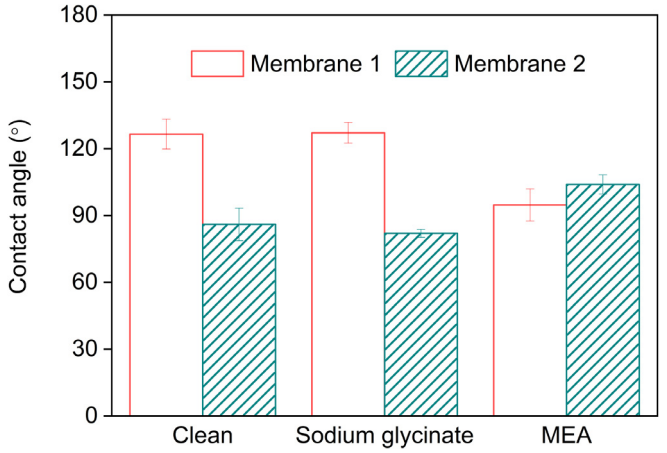

Fig. 3. Contact angles of membranes before and after the DCMD process (30% water recovery). Error bars represent the standard deviation of five repetitive measurements.

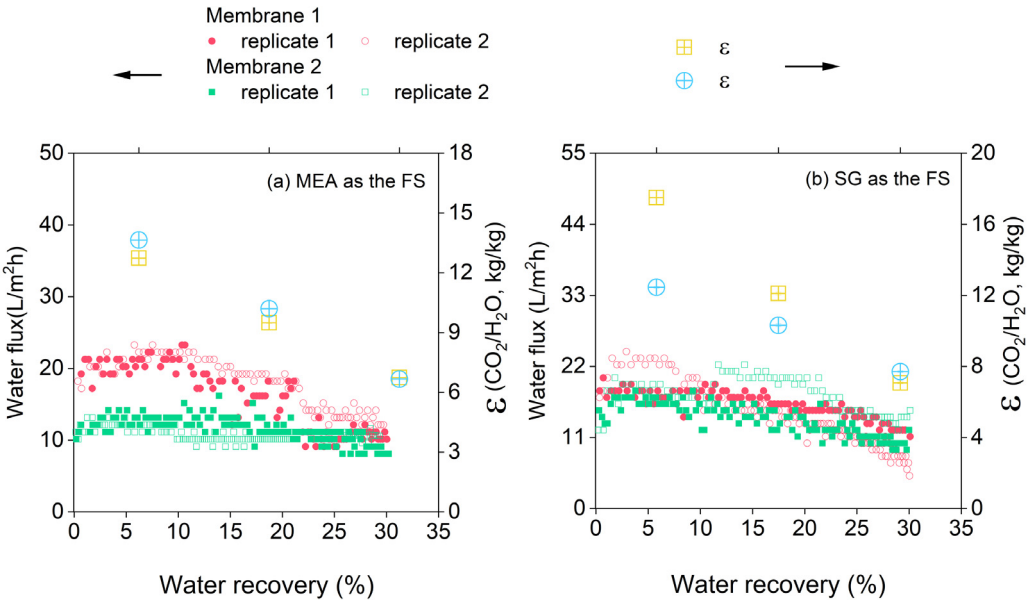

Fig. 4. Water flux and ratios of removed CO_2 and condensed water by DCMD during CO_2 desorption using different adsorbent: (a) MEA and (b) SG. Experimental conditions are described in Fig. 2.

conduction. This observation was also possibly due to the different hydrophobicity between these two membranes (Fig. 3). Membrane hydrophobicity appears to be a determining factor of the water flux trend for DCMD with MEA regeneration.

When sodium glycinate was used as the absorbent, both membranes showed a similar and more flux decline compared to MEA (Fig. 4b) despite the difference in their initial hydrophobicity. Exposure to sodium glycinate did not significantly alter the membrane hydrophobicity (Fig. 3). Thus, most of this flux decline observed in Fig. 4b can be attributed to the increase in viscosity of the sodium glycinate solution as it becomes more concentrated (Shaikh et al., 2014).

The stable hydrophobicity of both membranes (Section 3.1.2) could prevent the penetration of sodium glycinate through membrane pore into distillate, thus, maintaining high distillate quality. This is consistent with the high solute rejection (>98%) observed for amines in this study (Supplementary data Fig. S2). Given the high rejection of MEA and sodium glycinate by DCMD, amine loss during the CO_2 desorption can be avoided.

The ratio of CO_2 removed over water condensed, ε, can be considered as an indicator of the energy requirement. In Fig. 4, ε declined as a function of water recovery when both amines were used as the feed. Water condensed led to the increasing concentration of amine solution, which constrain the CO_2 desorption. Due to a higher carbamate stability, MEA showed a lower ε than sodium glycinate at the same water recovery. Associated with the decreasing CO_2 loading, both membranes showed high amine rejection (>98%) (Supplementary data Fig. S2).

Table 2
Concentration of MEA and sodium glycinate in feed and distillate. Error bars represent the difference of two replicate measurements.

Membrane	MEA as the feed solution			Sodium glycinate as the feed solution		
	Feed (g/L)	Distillate (g/L)	Rejection (%)	Feed (g/L)	Distillate (g/L)	Rejection (%)
1	43.4 ± 3.5	0.3 ± 0.0	99.3 ± 0.0	18.4 ± 2.8	0.21 ± 0.03	98.9 ± 0.1
2	43.9 ± 5.2	0.8 ± 0.1	98.1 ± 0.2	18.8 ± 1.9	0.10 ± 0.02	99.5 ± 0.1

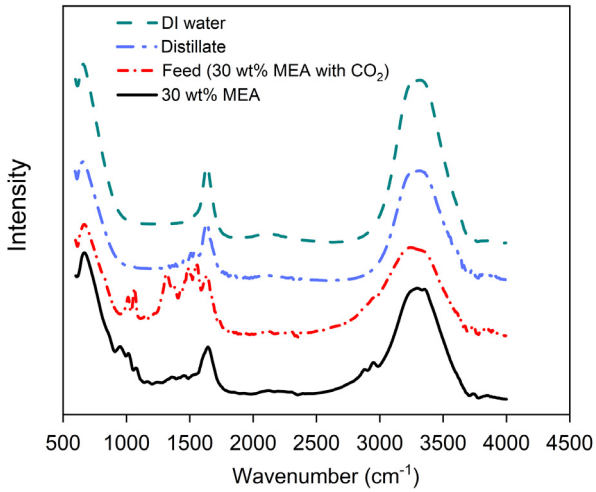

Fig. 5. Infrared spectra of the aqueous 30 wt % MEA (black line), feed solution: aqueous MEA at 0.59 mol/mol CO_2 loading (red line), distillate from the DCMD process (blue line), DI water as the reference (green line). (For interpretation of the references to colour in this figure legend, the reader is referred to the web version of this article.)

3.1.4. Amine loss in the DCMD distillate

TOC measurement shows no discernible increase in carbon content of the distillate, indicating no or negligible amine loss to the distillate by the DCMD process (Table 2). FTIR was used to further examine amine loss to the distillate being a reliable analytical technique to monitor the chemical reaction due to the measurable change of a molecule's dipole moment in the mid-IR region (400–4000 cm^{-1}). It is to be noted that peaks appearing between 3000 and 4000 cm^{-1} provided information unrelated to chemical reaction between CO_2 and amine. This is because that hydrogen bonding and O–H stretching of H_2O resulted in some broad peaks between 3200 and 3700 cm^{-1}. In addition, other chemical bonds (i.e. N–H, C–H, and O–H) stretching also resulted in the particular peaks in this wide region. Thus, this region is known as "the hydrogen stretching region", which is not included in our further discussion.

The infrared spectra of aqueous MEA prior to/after CO_2 absorption are given in Fig. 5. Several characteristic vibration modes appeared prior to CO_2 absorption, for example, C–N–H out-of-plane bending and C-NH_2 twisting at 950 cm^{-1}, C–O stretching at 1016 cm^{-1}, and C–N stretching at 1076 cm^{-1}, and N–H rocking at 1645 cm^{-1} (Richner and Puxty, 2012). After molecular CO_2 dissolving into MEA, several peaks shifted due to the protonation of the MEA and formation of carbamate and bicarbonate. Specifically, N-COO^- stretching vibration was observed at 1319 cm^{-1}. COO^- symmetric and asymmetric stretching occurred at 1486 and 1568 cm^{-1}, respectively (Richner and Puxty, 2012; Robinson et al., 2011). As reported by Richner and Puxty (Richner and Puxty, 2012), the variation in peak intensity was indicated by the difference of CO_2 loading in aqueous MEA. Shifting peaks was therefore not expected to occur after desorption.

The infrared spectra of distillate and DI water were compared to validate the high rejection for DCMD (Fig. 5). These results were consistent with data obtained in supplementary data Fig. S2. The spectrum of distillate was identical to that of DI water in spite of several negligible peaks between 1500 and 1568 cm^{-1}. This observation indicated that small amounts of carbamates had penetrated through membrane pore via water vapour. Unlike MEA, sodium glycinate can hardly vaporise as a salt even at a high temperature.

3.2. Make-up water by FO

The regenerated amines were used as the draw solution to obtain make-up water from secondary treated effluent. The water flux was stable and membrane fouling was not observed when either MEA or sodium glycinate was the draw solution (Fig. 6). It is noteworthy that the initial concentrations of MEA and sodium glycinate for CO_2 adsorption were 5 and 3 M, respectively (Section 2.2). Despite this difference in concentration, they resulted in the same water flux of 15 L/m^2h. This is because MEA and sodium glycinate are not ideal electrolytes. As elucidated in a previous study, the osmotic pressure does not increase linearly as the concentration increase and there is a threshold concentration at which

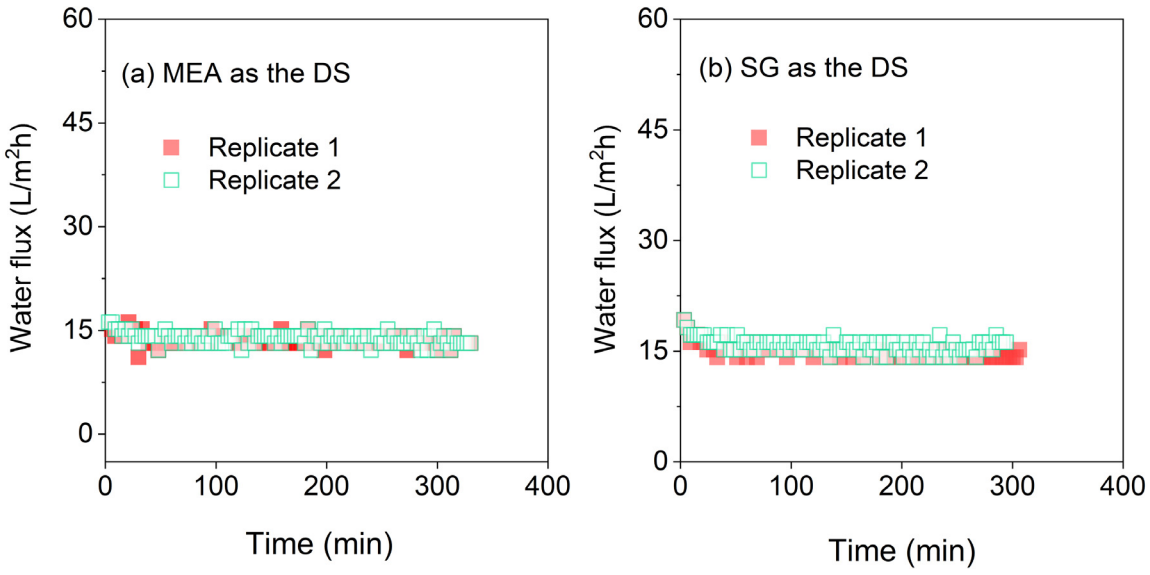

Fig. 6. Water flux profile of the FO process for regenerated amine solutions versus treated effluent: (a) MEA at 5M as the draw solution (DS); (b) Sodium glycinate at 3M as the DS. Feed solution (FS) and DS were circulated in the counter-current direction. Replicate experiments were conducted in AL-DS membrane orientation until 30% water recovery.

Table 3
CO_2 loading α from selected amine solutions in the different stage of experiment. Treated effluent and DI water were used as the cooling sources, unit: mol CO_2/mol amine.

Selected solution	1st cycle CO_2 absorption	1st cycle CO_2 desorption	Desorption efficiency	2nd cycle of CO_2 absorption (after FO)	Re-adsorption efficiency
MEA	0.54	0.36	33.3%	0.47	87.0%
SG	0.59	0.39	33.9%	0.52	88.1%

the osmotic pressure does not increase any further (Zheng et al., 2020). This result necessitates further investigation in terms of water flux optimisation. The FO process also provides cooling to the generated amine solution although it is beyond the scope of this current study.

3.3. Repetitive CO_2 absorption by amine solutions after desorption

Repetitive CO_2 absorption and desorption performance for both MEA and sodium glycinate by the MD–FO process is summarised in Table 3. In the first cycle, MEA exhibited the 33.3% CO_2 desorption efficiency with sodium glycinate slightly higher at 33.9%. Due to the high rejection of FO process (supplementary data Fig. S3), treated effluent could provide adequately clean water to cool down the heated amine solution for repetitive absorption. MEA and sodium glycinate also showed similar re-absorption efficiency of 87.0% and 88.1%, respectively. The observed re-absorption efficiency of below 100% in the 2nd cycle highlight the need for further investigation since in a practical application, the performance must be stable over thousands of cycles. It is noteworthy that amine loss from MD desorption was insignificant (Section 3.1.4). Thermal degradation was also expected to be negligible given the low desorption temperature (~80 °C) in this study.

3.4. Future work for practical applications

The proposed MD–FO process has shown some initial and promising results for the repetitive amine-based CO_2 capture from flue gas. Results reported in this study also highlight several technical challenges for further research and development. Future research work is recommended to include the screening of other commercially available amine solutions for CO_2 desorption by the MD system. Their respective CO_2 desorption and degradation are important parameters to assess their practical applications in the MD system. Further FO membrane development is recommended to limit the reverse salt flux for low or zero amine loss and stable water flux during the cooling process. A techno-economic analysis of the integrated system including the overall energy consumption requirement is also necessary to evaluate the potential of our proposed MD–FO process for practical applications.

4. Conclusion

This study demonstrated an integrated MD–FO system for the continuous CO_2 capture. MD–FO simultaneously provides low temperature CO_2 desorption and trim cooling as a promising alternative to utilise waste heat and treated effluent in power plants. The MD process achieved 33.6% and 33.2% CO_2 desorption efficiency for MEA and sodium glycinate at 80 °C, respectively. Interaction between amine adsorbent and the MD membrane could alter the membrane surface contact angle with water but under all experimental conditions, it was sufficiently hydrophobic for MD operation. Amine loss during CO_2 desorption by MD was insignificant. The regenerated MEA and sodium glycinate exhibited stable FO water flux for make-up water provision when secondary treated effluent was used as the feed. The results also highlight a major technical challenge for further investigation. Repetitive CO_2 loading and desorption showed less than 90% CO_2 re-absorption efficiency for either MEA or sodium glycinate in the second cycle. It is necessary to delineate the reason for this incomplete re-adsorption in a future study. Although this study is still preliminary, it provides important experimental data for further development of a novel membrane-based platform for CO_2 capture from flue gas.

CRediT authorship contribution statement

Lei Zheng: Conceptualization, Methodology, Investigation, Data Curation, Writing-Original Draft, Writing - Review & Editing. **Kangkang Li:** Resources, Data Curation, Visualization, Writing - Review & Editing. **Qilin Wang:** Supervision, Writing-Review & Editing. **Gayathri Naidu:** Visualization, Writing - Review & Editing. **William E. Price:** Supervision, Writing - Review & Editing. **Xiwang Zhang:** Methodology, Writing - Review & Editing. **Long D. Nghiem:** Conceptualization, Resource, Visualization, Supervision, Project administration, Funding acquisition, Writing - Review & Editing.

Declaration of competing interest

The authors declare that they have no known competing financial interests or personal relationships that could have appeared to influence the work reported in this paper.

Acknowledgements

The authors thank the financial support from the Australian Research Council through the ARC Research Hub for Energy-efficient Separation (IH170100009). Lei Zheng would like to express his gratitude to Faculty of Engineering and Information Technology (FEIT), University of Technology Sydney (UTS) for awarding him a FEIT PhD Post-Thesis Publication Award. His gratitude also goes to China Scholarship Council and UTS for the provision of a doctoral scholarship. Mr Minh Vu is acknowledged for his help in FTIR analysis.

Appendix A. Supplementary data

Supplementary material related to this article can be found online at https://doi.org/10.1016/j.eti.2021.101508.

References

Ahmad, N.A., Leo, C.P., Ahmad, A.L., 2018. Amine wetting evaluation on hydrophobic silane modified polyvinylidene fluoride/silicoaluminophosphate zeolite membrane for membrane gas absorption. J. Nat. Gas Sci. Eng. 58, 115–125.

Aroonwilas, A., Tontiwachwuthikul, P., 1998. Mass transfer coefficients and correlation for CO_2 absorption into 2-amino-2-methyl-1-propanol (AMP) using structured packing. Ind. Eng. Chem. Res. 37, 569–575.

Barzagli, F., Giorgi, C., Mani, F., Peruzzini, M., 2018. Reversible carbon dioxide capture by aqueous and non-aqueous amine-based absorbents: A comparative analysis carried out by 13C NMR spectroscopy. Appl. Energy 220, 208–219.

Barzagli, F., Giorgi, C., Mani, F., Peruzzini, M., 2019. Comparative study of CO_2 capture by aqueous and nonaqueous 2-amino-2-methyl-1-propanol based absorbents carried out by ^{13}C NMR and enthalpy analysis. Ind. Eng. Chem. Res. 58, 4364–4373.

Barzagli, F., Mani, F., Peruzzini, M., 2013. Efficient CO_2 absorption and low temperature desorption with non-aqueous solvents based on 2-amino-2-methyl-1-propanol (AMP). Int. J. Greenhouse Gas Control 16, 217–223.

Caplow, M., 1968. Kinetics of carbamate formation and breakdown. J. Am. Chem. Soc. 90, 6795–6803.

Cheng, C.-h., Li, K., Yu, H., Jiang, K., Chen, J., Feron, P., 2018. Amine-based post-combustion CO_2 capture mediated by metal ions: Advancement of CO_2 desorption using copper ions. Appl. Energy 211, 1030–1038.

Duong, H.C., Chivas, A.R., Nelemans, B., Duke, M., Gray, S., Cath, T.Y., Nghiem, L.D., 2015. Treatment of RO brine from CSG produced water by spiral-wound air gap membrane distillation — A pilot study. Desalination 366, 121–129.

Dutcher, B., Fan, M., Russell, A.G., 2013. Amine-based CO_2 capture technology development from the beginning of 2013—A review. ACS Appl. Mater. Interfaces 7, 2137–2148.

Feron, P., Thiruvenkatachari, R., Cousins, A., 2017. Water production through CO_2 capture in coal-fired power plants. Energy Sci. Eng. 5, 244–256.

Gingerich, D.B., Mauter, M.S., 2015. Quantity, quality, and availability of waste heat from United States thermal power generation. Environ. Sci. Technol. 49, 8297–8306.

Guo, D., Thee, H., Tan, C.Y., Chen, J., Fei, W., Kentish, S., Stevens, G.W., da Silva, G., 2013. Amino acids as carbon capture solvents: Chemical kinetics and mechanism of the glycine + CO_2 reaction. Energy Fuels 27, 3898–3904.

Gwak, G., Kim, D.I., Kim, J., Zhan, M., Hong, S., 2019. An integrated system for CO_2 capture and water treatment by forward osmosis driven by an amine-based draw solution. J. Membr. Sci. 581, 9–17.

Hamborg, E.S., van Aken, C., Versteeg, G.F., 2010. The effect of aqueous organic solvents on the dissociation constants and thermodynamic properties of alkanolamines. Fluid Phase Equilib. 291, 32–39.
Idem, R., Wilson, M., Tontiwachwuthikul, P., Chakma, A., Veawab, A., Aroonwilas, A., Gelowitz, D., 2006. Pilot plant studies of the CO_2 capture performance of aqueous MEA and mixed MEA/MDEA solvents at the university of regina CO_2 capture technology development plant and the boundary dam CO_2 capture demonstration plant. Ind. Eng. Chem. Res. 45, 2414–2420.
Jia, W., Kharraz, J.A., Choi, P.J., Guo, J., Deka, B.J., An, A.K., 2020. Superhydrophobic membrane by hierarchically structured PDMS-POSS electrospray coating with cauliflower-shaped beads for enhanced MD performance. J. Membr. Sci. 597, 117638.
Lai, Q., Kong, L., Gong, W., Russell, A.G., Fan, M., 2019. Low-energy-consumption and environmentally friendly CO_2 capture via blending alcohols into amine solution. Appl. Energy 254, 113696.
Li, K., Cousins, A., Yu, H., Feron, P., Tade, M., Luo, W., Chen, J., 2016a. Systematic study of aqueous monoethanolamine-based CO_2 capture process: model development and process improvement. Energy Sci. Eng. 4, 23–39.
Li, K., Feron, P.H.M., Jones, T.W., Jiang, K., Bennett, R.D., Hollenkamp, A.F., 2020. Energy harvesting from amine-based CO_2 capture: proof-of-concept based on mono-ethanolamine. Fuel 263, 116661.
Li, K., Leigh, W., Feron, P., Yu, H., Tade, M., 2016b. Systematic study of aqueous monoethanolamine (MEA)-based CO_2 capture process: Techno-economic assessment of the MEA process and its improvements. Appl. Energy 165, 648–659.
Li, K., van der Poel, P., Conway, W., Jiang, K., Puxty, G., Yu, H., Feron, P., 2018. Mechanism investigation of advanced metal–ion–mediated amine regeneration: A novel pathway to reducing CO_2 reaction enthalpy in amine-based CO_2 capture. Environ. Sci. Technol. 52, 14538–14546.
Li, Y., Wang, L.a., Tan, Z., Zhang, Z., Hu, X., 2019. Experimental studies on carbon dioxide absorption using potassium carbonate solutions with amino acid salts. Sep. Purif. Technol. 219, 47–54.
Lin, P.-H., Wong, D.S.H., 2014. Carbon dioxide capture and regeneration with amine/alcohol/water blends. Int. J. Greenhouse Gas Control 26, 69–75.
Liu, S., Ling, H., Lv, J., Gao, H., Na, Y., Liang, Z., 2019. New insights and assessment of primary alkanolamine/sulfolane biphasic solutions for post-combustion CO_2 capture: Absorption, desorption, phase separation, and technological process. Ind. Eng. Chem. Res. 58, 20461–20471.
Luis, P., Van Gerven, T., Van der Bruggen, B., 2012. Recent developments in membrane-based technologies for CO_2 capture. Prog. Energy Combust. Sci. 38, 419–448.
Lv, B., Guo, B., Zhou, Z., Jing, G., 2015. Mechanisms of CO_2 capture into monoethanolamine solution with different CO_2 loading during the absorption/desorption processes. Environ. Sci. Technol. 49, 10728–10735.
McGurk, S.J., Martín, C.F., Brandani, S., Sweatman, M.B., Fan, X., 2017. Microwave swing regeneration of aqueous monoethanolamine for post-combustion CO_2 capture. Appl. Energy 192, 126–133.
Moioli, S., Pellegrini, L.A., Ho, M.T., Wiley, D.E., 2019. A comparison between amino acid based solvent and traditional amine solvent processes for CO_2 removal. Chem. Eng. Res. Des. 146, 509–517.
Naidu, G., Tijing, L., Johir, M.A.H., Shon, H., Vigneswaran, S., 2020. Hybrid membrane distillation: Resource, nutrient and energy recovery. J. Membr. Sci. 599, 117832.
Nguyen, L.N., Truong, M.V., Nguyen, A.Q., Johir, M.A.H., Commault, A.S., Ralph, P.J., Semblante, G.U., Nghiem, L.D., 2020. A sequential membrane bioreactor followed by a membrane microalgal reactor for nutrient removal and algal biomass production. Environ. Sci.: Water Res. Technol. 6, 189–196.
Novek, E.J., Shaulsky, E., Fishman, Z.S., Pfefferle, L.D., Elimelech, M., 2016. Low-temperature carbon capture using aqueous ammonia and organic solvents. Environ. Sci. Technol. Lett. 3, 291–296.
Peters, G.P., Andrew, R.M., Canadell, J.G., Friedlingstein, P., Jackson, R.B., Korsbakken, J.I., Le Quéré, C., Peregon, A., 2019. Carbon dioxide emissions continue to grow amidst slowly emerging climate policies. Nature Clim. Change.
Petra Nova - W.A. Parish Project in, 2018. Office of fossil energy.
Rabensteiner, M., Kinger, G., Koller, M., Gronald, G., Unterberger, S., Hochenauer, C., 2014. Investigation of the suitability of aqueous sodium glycinate as a solvent for post combustion carbon dioxide capture on the basis of pilot plant studies and screening methods. Int. J. Greenhouse Gas Control 29, 1–15.
Rahim, N.A., Ghasem, N., Al-Marzouqi, M., 2015. Absorption of CO_2 from natural gas using different amino acid salt solutions and regeneration using hollow fiber membrane contactors. J. Nat. Gas Sci. Eng. 26, 108–117.
Ray, S.S., Gandhi, M., Chen, S.-S., Chang, H.-M., Dan, C.T.N., Le, H.Q., 2018. Anti-wetting behaviour of a superhydrophobic octadecyltrimethoxysilane blended PVDF/recycled carbon black composite membrane for enhanced desalination. Environ. Sci.: Water Res. Technol. 4, 1612–1623.
Rezaiyan, Z., Keshavarz, P., Khorram, M., 2017. Experimental investigation of the effects of different chemical absorbents on wetting and morphology of poly(vinylidene fluoride) membrane. J. Appl. Polym. Sci. 134, 45543.
Richner, G., Puxty, G., 2012. Assessing the chemical speciation during CO_2 absorption by aqueous amines using in situ FTIR. Ind. Eng. Chem. Res. 51, 14317–14324.
Robinson, K., McCluskey, A., Attalla, M.I., 2011. An FTIR spectroscopic study on the effect of molecular structural variations on the CO_2 absorption characteristics of heterocyclic amines. ChemPhysChem 12, 1088–1099.
Rochelle, G.T., 2009. Amine scrubbing for CO_2 capture. Science 325, 1652.
Shaikh, M.S., Shariff, A.M., Bustam, M.A., Murshid, G., 2014. Analysis of physicochemical properties of aqueous sodium glycinate (SG) solutions at low concentrations from 0.1-2.0 M. J. Appl. Sci. 14, 1055–1060.
Singh, P., Versteeg, G.F., 2008. Structure and activity relationships for CO_2 regeneration from aqueous amine-based absorbents. Process Saf. Environ. Protect. 86, 347–359.
Song, L., Ma, Z., Liao, X., Kosaraju, P.B., Irish, J.R., Sirkar, K.K., 2008. Pilot plant studies of novel membranes and devices for direct contact membrane distillation-based desalination. J. Membr. Sci. 323, 257–270.
Song, H.-J., Park, S., Kim, H., Gaur, A., Park, J.-W., Lee, S.-J., 2012. Carbon dioxide absorption characteristics of aqueous amino acid salt solutions. Int. J. Greenhouse Gas Control 11, 64–72.
Stéphenne, K., 2014. Start-up of world's first commercial post-combustion coal fired CCS project: Contribution of shell cansolv to saskpower boundary dam ICCS project. Energy Procedia 63, 6106–6110.
Vevelstad, S.J., Eide-Haugmo, I., da Silva, E.F., Svendsen, H.F., 2011. Degradation of MEA; a theoretical study. Energy Procedia 4, 1608–1615.
Wang, P., Chung, T.-S., 2015. Recent advances in membrane distillation processes: Membrane development, configuration design and application exploring. J. Membr. Sci. 474, 39–56.
Xiao, Z., Guo, H., He, H., Liu, Y., Li, X., Zhang, Y., Yin, H., Volkov, A.V., He, T., 2020. Unprecedented scaling/fouling resistance of omniphobic polyvinylidene fluoride membrane with silica nanoparticle coated micropillars in direct contact membrane distillation. J. Membr. Sci. 599, 117819.
Xie, K., Fu, Q., Qiao, G.G., Webley, P.A., 2019. Recent progress on fabrication methods of polymeric thin film gas separation membranes for CO_2 capture. J. Membr. Sci. 572, 38–60.
Zhang, Z., Li, Y., Zhang, W., Wang, J., Soltanian, M.R., Olabi, A.G., 2018. Effectiveness of amino acid salt solutions in capturing CO_2: A review. Renew. Sustain. Energy Rev. 98, 179–188.
Zhang, X., Zhang, X., Liu, H., Li, W., Xiao, M., Gao, H., Liang, Z., 2017. Reduction of energy requirement of CO_2 desorption from a rich CO_2-loaded MEA solution by using solid acid catalysts. Appl. Energy 202, 673–684.

Zhao, Y., Bian, Y., Li, H., Guo, H., Shen, S., Han, J., Guo, D., 2017. A comparative study of aqueous potassium lysinate and aqueous monoethanolamine for postcombustion CO_2 capture. Energy Fuels 31, 14033–14044.
Zhao, S., Cao, C., Wardhaugh, L., Feron, P.H.M., 2015. Membrane evaporation of amine solution for energy saving in post-combustion carbon capture: Performance evaluation. J. Membr. Sci. 473, 274–282.
Zhao, S., Feron, P.H.M., Deng, L., Favre, E., Chabanon, E., Yan, S., Hou, J., Chen, V., Qi, H., 2016. Status and progress of membrane contactors in post-combustion carbon capture: A state-of-the-art review of new developments. J. Membr. Sci. 511, 180–206.
Zheng, L., Price, W.E., He, T., Nghiem, L.D., 2020. Simultaneous cooling and provision of make-up water by forward osmosis for post-combustion CO_2 capture. Desalination 476, 114215.